One-step hydrothermal fabrication of $AgInS_2/SnIn_4S_8$ nanocomposite with enhanced visible-light-activated photocatalytic activity

Fei Zhong[1], and *Zong Qiang* Zhu[1,2*]

[1]Guangxi Key Laboratory of Theory and Technology for Environmental Pollution Control, Guilin University of Technology, Guilin, 541006, China
[2]Collaborative Innovation Center for Water Pollution Control and Water Safety in Karst Area, Guilin University of Technology, Guilin, 541006, China

Abstract. In this experiment, $AgInS_2/SnIn_4S_8$ materials were prepared via one-step hydrothermal method using silver chloride, the indium trichloride, stannic chloride and thioacetamide as source of silver, indium, tin and sulfur sources, respectively. The structure, content and optical property of the as-synthesized $AgInS_2/SnIn_4S_8$ nanocomposite were investigated by powder X-ray diffraction, energy dispersive X-ray spectroscopy, field emission scanning electron microscopy.The ratio of $AgInS_2$ to $SnIn_4S_8$ was optimized. When the molar amount of $AgInS_2$ to $SnIn_4S_8$ is 0.6, $AgInS_2/SnIn_4S_8$ composite photocatalyst shows the highest photocatalytic activity for degrading 2-nitrophenol (2NP) due to large absorption range and visible-light response. $AgInS_2/SnIn_4S_8$ composites not only can degrade 2NP and tetracycline, but also had good mineralization efficiency for pharmaceutical industry wastewater.

1 Introduction

With the development of medicine, chemical dyes, rubber and other industries, more and more organic pollutants are discharged into the natural environment[1-3]. Although drugs can protect human beings from the invasion of germs, a large number of pollutants are discharged into the environment and cause serious pollution[4]. Antibiotics, hormones, preservatives, anesthetics, and other organic chemicals have been detected in drinking water, groundwater, and surface water[5-9]. During the medication production stage, pharmaceutical factories will release a large number of intermediate products into pharmaceutical wastewater as by-products[10-12. If wastewater released into the natural environment, they will seriously pollute water supplies. Many studies attempt to use photocatalysis technology to break down organic materials in order to mitigate these organic pollutants. By using the photocatalyst's REDOX capability, photocatalysis technology breaks down organic matter into safe intermediates using sunlight as an excitation source[13-15].

Photocatalysis technique is more cost-effective, practical, and ecologically benign than conventional sewage treatment methods[16-18]. It has been found that the ternary metal

*Corresponding author: 1107328169@qq.com

sulfide $SnIn_4S_8$ has sufficient absorption of sunlight due to its narrow band gap, but its structure cannot prevent the recombination of photogenerated electron holes, which limits its application[19-20].

Representative ternary chalcogenide materials are $SnIn_4S_8$ and $AgInS_2$, and photocatalytic degradation of organic contaminants triggered by visible light has been extensively studied[21-23]. Sadly, the quick recombination of photogenerated electrons and holes typically leads to inadequate photocatalytic performance for a single semiconductor[24-27]. The construction of heterojunction photocatalyst can accelerate the interfacial charge transfer and reduce the photogenerated electron-hole pair recombination, thus improving the photocatalytic performance. Undoubtedly, the photocatalytic activity of pure ternary chalcogenide has been enhanced by the creation of heterojunction photocatalysts using additional semiconductors[28-30]. Further preparation of a more effective ternary chalcogenide heterojunction is still required to increase the practical application and photocatalytic efficiency

In this work, $AgInS_2/SnIn_4S_8$ nanocomposites were synthesized by one-step hydrothermal method, and the optimal ratio of $AgInS_2$ and $SnIn_4S_8$ was explored by regulating the component content of $AgInS_2$ and $SnIn_4S_8$. $SnIn_4S_8/AgInS_2$ heterojunction has good photocatalytic degradation effect on 2NP. In addition, the mineralization rate of 20 mg $AgInS_2/SnIn_4S_8$ heterojunction for 100 mL of wastewater from pharmaceutical production in the presence of H_2O_2 was 65.98%. At the same time, the chemical oxygen demand (COD) of the wastewater from pharmaceutical production was reduced to 153 mg/L, reaching the industrial wastewater discharge standard.

2 Experimental details

2.1 Chemicals

Deionized water was utilized in the experiment.All reagents and solutions are obtained from the supplier and are not processed further. Anhydrous sodium sulfate (Na_2SO_4) and anhydrous ethanol (C_2H_6O) were obtained from Sinopharm Chemical Reagent Co., Ltd. (Shanghai, China). Tin (IV) chloride pentahydrate ($SnCl_4·5H_2O$, AR) and indium trichloride tetrahydrate ($InCl_3·4H_2O$, AR) was supplied by Aladdin Biochemical Technology Co., Ltd. (Shanghai, China). Analytical grade o-nitrophenol($C_6H_5NO_3$), thioacetamide (TAA, AR) was received from Shantou Xilong Chemical Co., Ltd. (Shantou, China).

2.2 Sample preparation

$AgInS_2/SnIn_4S_8$ composites with different molar ratios were prepared by a simple one-step hydrothermal method. Before the experiment, 5 g $InCl_3$ was dissolved in a 50 mL beaker and then transferred to a 100 mL volumetric bottle to obtain 50 g/L $InCl_3$ solution. Since the indium salt out of the $InCl_3$ solution over time, use the $InCl_3$ solution immediately. Firstly, $AgNO_3$, SnCl4·$5H_2O$ is magnetically stirred in a 50 mL beaker with 19.5 mL deionized water and 10.5 mL of the previously prepared $InCl_3$ solution until the solid is completely dissolved. Then, add thioacetamide (TAA) and continue stirring for 30 min to make the solution evenly mixed. Finally, the mixed solution was transferred to a 50 mL reactor and reacted at 180°C for 12 hours. Following the reaction, impurity ions were eliminated from the samples by repeatedly washing them in alcohol. The products were then recovered by centrifugation. Following washing, the samples were vacuum-dried for 12 hours at 60 °C.

2.3 Characterization

X-ray diffraction (XRD) analysis was performed on a Bruker D/MAX-B X-ray diffractometer. The morphology of pure $AgInS_2$, $SnIn_4S_8$ and (0.6:1) $AgInS_2/SnIn_4S_8$ composites was investigated by scanning electron microscopy. Total organic carbon (TOC) was determined by the multi N/C® 2100 analyzer (Analytik Jena AG, Germany).

2.4 Evaluation of photocatalytic activity

The 20 mg photocatalyst was weighed into a 150 mL beaker and 100 mL 10 mg/L o-nitrophenol (2NP) was added. To fully mix the solution and achieve the equilibrium condition of adsorption and desorption, a 120-minute dark reaction was conducted prior to light irradiation. Three milliliters (mL) of the solution were extracted and designated as C_0 after the conclusion of the dark reaction. The remaining solution was then moved to visible light to undergo photocatalytic reaction.Every 20 minutes, a sample was collected, measured as C_t, and filtered using a drainage filter with a pore size of 0.45μm.The absorbance of the solution is measured, and then the concentration of pollutants in different time periods can be obtained according to Lamberbier's law. Finally, the degradation rate of 2NP by the catalyst is calculated. The pH of the solution was adjusted between 1 and 11 using 0.5 mol/L NaOH and 0.5 mol/L HCl in order to study the degradation of $AgInS_2/SnIn_4S_8$ complex at various pH levels.

3. Results and discussion

3.1 XRD Analysis

XRD analyses were performed to confirm the crystal structure of $AgInS_2/SnIn_4S_8$(seen in Figure 1). For pure $AgInS_2$ sample, five distinct diffraction peaks can be observed at 23.17°, 27.29°, 33.23°, 43.57° and 47.62°, which belonged to (220), (311), (400), (511) and (440) planes of $AgInS_2$ (PDF#26-1477). Pure $SnIn_4S_8$ shows of sharp diffraction peaks, which can be matched well to the tetragonal phase $SnIn_4S_8$ (PDF#42-1305). Because the peaks of the two substances are so close together, there are many summits that overlap. These results indicate that the $AgInS_2/SnIn_4S_8$ complex with good crystallinity can be obtained by a simple one-step hydrothermal method, and there is a strong interaction between $AgInS_2$ and $SnIn_4S_8$, which lays a foundation for the photocatalytic performance of the complex.

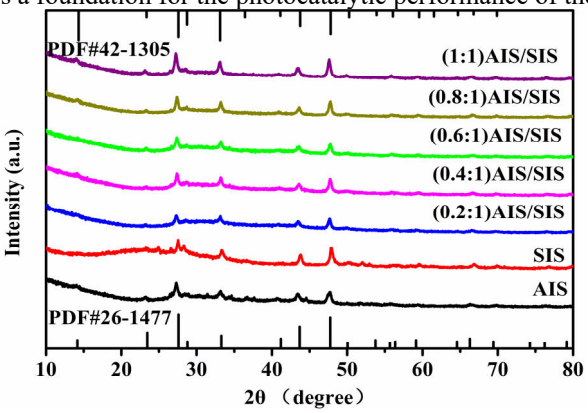

Fig. 1. XRD patterns of $AgInS_2$, $SnIn_4S_8$ and $AgInS_2/SnIn_4S_8$ heterojunctions with different molar ratio.

3.2 SEM analysis

From the Figure 2a, we can see that $AnInS_2$ is an irregular structure composed of stacked nanosheets, with large gaps between the sheets. $SnIn_4S_8$ consists of many nanoblocks of different shapes stacked together to form a three-dimensional structure(seen in Figure 2b), which is not conducive to the transfer of photogenic electrons. When $AnInS_2$ is combined with $SnIn_4S_8$, it is still composed of some lamellar structures, but its diameter is slightly larger than that of pure $AnInS_2$, and the thickness of nanosheets is between $AnInS_2$ and $SnIn_4S_8$.

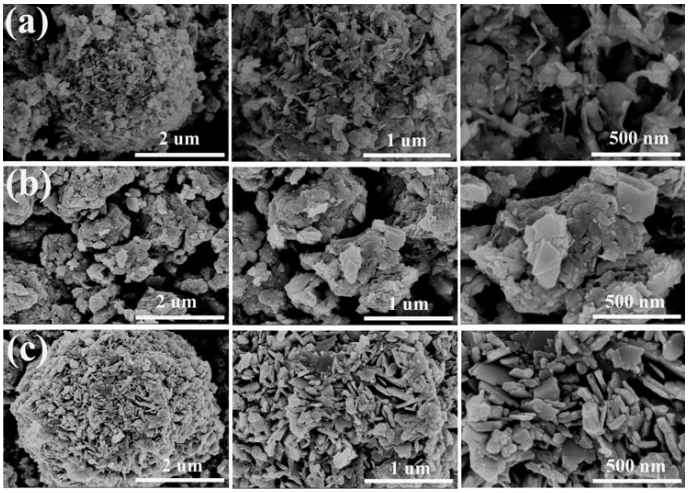

Fig. 2. SEM image of $AgInS_2$(a), $SnIn_4S_8$ (b) and (0.6:1)$AgInS_2/SnIn_4S_8$ composites.

3.3 Photocatalytic degradation of 2NP

It is known from the experimental results that the sample has obvious effect on the degradation of 2NP. The degradation rates of 2NP by $AgInS_2$, $SnIn_4S_8$, (0.2:1) $AgInS_2/SnIn_4S_8$, (0.4:1) $AgInS_2/SnIn_4S_8$, (0.6:1) $AgInS_2/SnIn_4S_8$, (0.8:1) $AgInS_2/SnIn_4S_8$ and (1:1) $AgInS_2/SnIn_4S_8$ were 52%, 50%, 73%, 89%, 92%, 78% and 76%, respectively. The photocatalytic degradation effect of $AgInS_2/SnIn_4S_8$ complex was significantly better than that of pure $AgInS_2$ and pure $SnIn_4S_8$, and the photocatalytic activity of the complex increased when the molar ratio of $AgInS_2$ to $SnIn_4S_8$ increased from 0.2 to 0.6 (Figure 3).

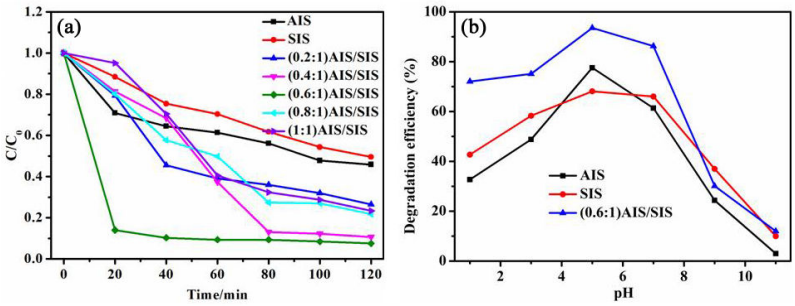

Fig. 3. (a)Photocatalytic degradation (b) photocatalytic degradation at different pH values.

3.4 Practical application of photocatalytic materials

The mineralized status of organic matter can be obtained by measuring the total organic carbon content in aqueous solution with the total organic carbon (TOC) analyzer. When 20mg (0.6:1)AIS/SIS photocatalytic material was added to 100 ml of wastewater, it was found that TOC value changed significantly. Figure 4a shows the change of TOC over time during the degradation of actual wastewater by (0.6:1)$AgInS_2/SnIn_4S_8$ composite material under visible light. After 6 hours of continuous illumination, TOC drops to 65.93%. When H_2O_2 and (0.6:1)AIS/SIS were present at the same time, the mineralization rate of pharmaceutical wastewater reached 65.98%.When 5 mL 30% H_2O_2 and 20 mg (0.6:1)AIS/SIS were added to pharmaceutical wastewater, the COD decreased from 634mg/L to 521 and 296.7 mg/L, respectively. Pharmaceutical wastewater's COD is lowered to 153 mg/L when AIS/SIS and H_2O_2 are applied simultaneously, meeting industrial wastewater discharge regulations.

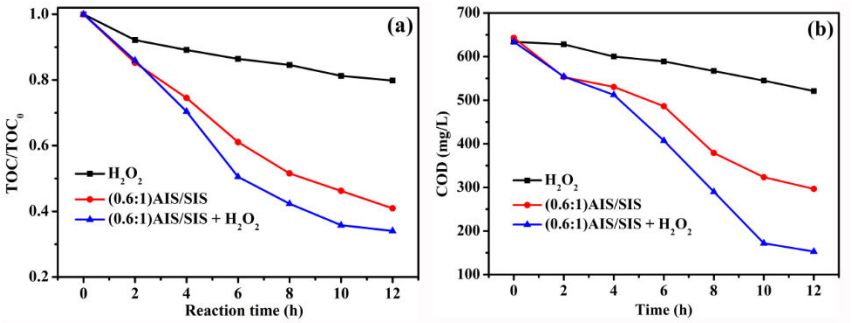

Fig. 4 (a)TOC and (b)COD results for H_2O_2, (0.6:1)$AgInS_2/SnIn_4S_8$ and (0.6:1) $AgInS_2/SnIn_4S_8$+5mLH_2O_2 photocatalytic degradation of 2NP under visible light irradiation.

4. Conclusions

Hydrothermal nanocomposites $AgInS_2/SnIn_4S_8$ were synthesized using a straightforward one-step process. When constructed with the proper molar ratio, the $AgInS_2/SnIn_4S_8$ heterojunction exhibits outstanding visible light photocatalytic degradation capability. Furthermore, actual pharmaceutical wastewater may be efficiently treated by the $AgInS_2/SnIn_4S_8$ heterojunction to satisfy discharge regulations.

References

1. S. Miralles-Cuevas, I. Oller, A. Agüera, M. Llorca, J.A. Sánchez Pérez, S. Malato , Combination of nanofiltration and ozonation for the remediation of real municipal wastewater effluents: acute and chronic toxicity assessment. J. Hazard. Mater. 323, 442-451 (2017).

2. X. Zhang, C. Chen, P. Lin, A. Hou, Z. Niu, J. Wang, Emergency drinking water treatment during source water pollution accidents in China: origin analysis, framework and technologies. Environ. Sci. Technol. **45**, 161 (2011).

3. R.P. Schwarzenbach, T. Egli, T.B. Hofstetter, U.V. Gunten, B. Wehrli, Global water pollution and human health. Annu. Rev. Env Resour. **35**,109−136 (2010).

4. L.Jun, W.Wu, Q.Y. Tian, Z.G. Dai, Z.H. Wu, X.H.Xiao, and C.Z.Jiang, Anchoring of

$Ag_6Si_2O_7$ nanoparticles on α-Fe_2O_3 short nanotubes as a Z-scheme photocatalyst for improving their photocatalytic performances. Dalton Trans. no. **32**, 12745-12755(2016).

5. G. Darabdhara, P.K. Boruah, P. Borthakur, N. Hussain, M.R. Das, T. Ahamad, S.M. Alshehri, V. Malgras, K.C. Wu, Y. Yamauchi, Reduced graphene oxide nanosheets decorated with Au–Pd bimetallic alloy nanoparticles towards efficient photocatalytic degradation of phenolic compounds in water. Nanoscale **8**, 8276-8287 (2016).

6. H. Cheng, B. Huang, Y. Dai, Engineering BiOX (X= Cl, Br, I) nanostructures for highly efficient photocatalytic applications. Nanoscale **4**, 2009-2026 (2014).

7. Y. Wang, Q. Wang, X. Zhan, F. Wang, M. Safdar, J. He, Visible light driven type II heterostructures and their enhanced photocatalysis properties: a review. Nanoscale **5**, 8326(2013).

8. X. Yang, W. Chen, J. Huang, Y. Zhou, Y. Zhu, C. Li, Rapid degradation of methylene blue in a novel heterogeneous Fe_3O_4@ rGO@ TiO_2-catalyzed photo-Fenton system. Scientific reports 5,10632 (2015).

9. H. Zhang, L.H. Guo, D. Wang, L. Zhao, B. Wan, Light-induced efficient molecular oxygen activation on a Cu (II)-grafted TiO_2/graphene photocatalyst for phenol degradation. ACS Appl. Mater. Interfaces.**7**, 1816 (2015).

10. X. Luo, F. Deng, L. Min, S. Luo, B. Guo, G. Zeng, C. Au, Facile one-step synthesis of inorganic-framework molecularly imprinted TiO_2/WO_3 nanocomposite and its molecular recognitive photocatalytic degradation of target contaminant. Environ. Sci. Technol. **47**, 7404-7412 (2013).

11. M. Niu, D. Cheng, D. Cao, SiH/TiO_2 and GeH/TiO_2 heterojunctions: Promising TiO_2-based photocatalysts under visible light.Sci Rep **4**, 4810 (2014).

12. T. Leijtens, G.E. Eperon, S. Pathak, A. Abate, M.M. Lee, H.J. Snaith, Overcoming ultraviolet light instability of sensitized TiO_2 with meso-superstructured organometal tri-halide perovskite solar cells. Nature Communications **4**, 2885 (2013).

13. Y. C. Zhang, L. Yao, G. S. Zhang, Dionysios D. Dionysiou ,J. Li, X.H. Du, One-step hydrothermal synthesis of high-performance visible-light-driven SnS_2/SnO_2 nanoheterojunction photocatalyst for the reduction of aqueous Cr (VI). Appl Catal B: Environ. **144**, 730– 738(2014).

14. Y. C. Zhang , Q. Zhang, Q. W. Shi, Z. Y. Cai, Z. J. Yang. Acid-treated g-C_3N_4 with improved photocatalytic performance in the reduction of aqueous Cr (VI) under visible-light. Separation and Purification Technology **142**, 251–257 (2015).

15. Y. C. Zhang, M. Yang, G. S. Zhang, Dionysios D. Dionysiou. HNO_3-involved one-step low temperature solvothermal synthesis of N-doped TiO_2 nanocrystals for efficient photocatalytic reduction of Cr (VI) in water. Appl Catal B: Environ. **142**, 249–258(2013).

16. L. Wang, X. Li, W. Teng, Q. Zhao, Y. Shi, R. Yue, Y. Chen, Efficient photocatalytic reduction of aqueous Cr (VI) over flower-like $SnIn_4S_8$ microspheres under visible light illumination. J. Hazard. Mater. **244**, 681-688 (2013).

17. S.K. Batabyal, S.E. Lu, J.J. Vittal, Synthesis, characterization, and photocatalytic properties of In_2S3, $ZnIn_2S_4$, and CdIn2S4 nanocrystals. Crystal Growth & Design **16**

(2016).

18. S. Jeong, H.C. Yoon, N.S. Han, H.O. Ji, S.M. Park, B.K. Min, Y.R. Do, J.K. Song, band-gap states of $AgIn_5S_8$ and ZnS–$AgIn_5S_8$ nanoparticles. J. Phys. Chem. C **121**, 3149−3155(2017).

19. S. Shen, L. Li, Z. Wu, M. Sun, Z. Tang, J. Yang, In_4SnS_8 ultrathin nanosheets: a ternary sulfide with fast adsorption–visible-light photocatalysis dual function. RSC Adv. **7**, 4555(2017).

20. T. Yan, L. Li, G. Li, Y. Wang, W. Hu, X. Guan, Porous $SnIn_4S_8$ microspheres in a new polymorph that promotes dyes degradation under visible light irradiation. J. Hazard. Mater. **186**, 272-279(2011).

21. F. Deng, F. Zhong, P. Hu, X. Pei, X. Luo, S. Luo, Fabrication of In-rich $AgInS_2$ nanoplates and nanotubes by a facile low-temperature co-precipitation strategy and their excellent visible-light photocatalytic mineralization performance. Journal of Nanoparticle Research. **19**, 14 (2017).

22. B. Mao, C.H. Chuang, J. Wang, C. Burda, Synthesis and photophysical properties of ternary I–III–VI $AgInS_2$ nanocrystals: intrinsic versus surface states. J. phys. chem.c **115**, 8945-8954 (2011).

23. T. Yan, L. Li, G. Li, Solvothermal synthesis of hierarchical $SnIn_4S_8$ microspheres and their application in photocatalysis. Res Chem Intermed. **37**, 297-307 (2011).

24. Y. Hamanaka, T. Ogawa, M. Tsuzuki, T. Kuzuya, Photoluminescence properties and its origin of $AgInS_2$ quantum dots with chalcopyrite structure. Journal of Physical Chemistry C. **115**, 1786-1792 (2011).

25. Z. Wang, J. Zhang, J. Lv, K. Dai, C. Liang, Plasmonic Ag_2MoO_4/AgBr/Ag composite: excellent photocatalytic performance and possible photocatalytic mechanism. Appl. Surf. Sci. **396**, 791-798 (2017)

26. S. Shenawikhalil, V. Uvarov, S. Fronton, I. Popov, Y. Sasson, A novel heterojunction BiOBr/bismuth oxyhydrate photocatalyst with highly enhanced visible light photocatalytic properties. J. Phys. Chem. C. **116**, 11004-11012 (2012).

27. Y. Yu, Y. Tang, J. Yuan, Q. Wu, W. Zheng, Y. Cao, Fabrication of N-TiO_2/$InBO_3$ heterostructures with enhanced visible photocatalytic performance. J. Phys. Chem. C. **118**, 13545–13551 (2014).

28. K. Li, B. Chai, T. Peng, J. Mao, L. Zan, Preparation of $AgIn_5S_8$/TiO_2 Heterojunction Nanocomposite and Its Enhanced Photocatalytic H_2 Production Property under Visible Light ACS Catalysis. **3**, 170–177 (2013).

29. T. Wang, Y. Zhang, T. Ding, One-step solvothermal synthesis of $SnIn_4S_8$/TiO_2 nanocomposite with enhanced visible-light-activated photocatalytic activity. Materials Letters. **123**, 153-155 (2014).

30. B. Liu, X. Li, Q. Zhao, J. Ke, M. Tadé, S. Liu, Preparation of $AgInS_2$/TiO_2 composites for enhanced photocatalytic degradation of gaseous o-dichlorobenzene under visible light. Appl Catal B: Environ. **185**, 1-10 (2016).